

A new set of focused wave linear combinations to extract non-linear wave harmonics

by Martyn Hann^{*}, Deborah Greaves and Alison Raby
 School of Marine Science and Engineering, Plymouth University, PL4 8AA, UK
 E-mail: martyn.hann@plymouth.ac.uk

Highlights:

- A new set of linear combinations of New-wave type focused waves of different phases is presented to extract linear and higher order harmonic components from a Stokes-type expansion of surface elevation.
- Experimental measurements are presented confirming that the new combinations proposed here and those previously published [1] are equivalent up to 4th order.

1 Introduction

Results are reported from a series of experimental measurements using NewWave type uni-directional wave groups to generate extreme loads on a single taut-moored hemispherical float. Twelve wave groups have been tested, each with a different phase at the focus location (0° to 330° in 30° intervals). Fitzgerald et al. [1] and Siddorn [2] use a linear combination of wave groups to separate linear and nonlinear harmonics of surface elevation. Here an alternative set of wave group combinations is introduced that remove the need for frequency filtering. The NewWave groups [3] were generated with a crest amplitude (A_n) of 0.267 m and an underlying Pierson Moskowitz (PM) spectrum with a peak frequency of 0.356 Hz. These values represent a 100 year storm at 50th scale and are derived from hindcast data for the Wave Hub renewable energy test facility off the south west UK coast (Halcrow [4] p. 19).

2 Experimental set-up

Measurements were conducted in the 35m long x 15.5m wide ocean basin in Plymouth University's COAST laboratory (www.plymouth.ac.uk/coast). The variable floor depth was set to 2.8 m and the float was moored 20.9 m from the front edge of the 24 wave paddles. A parabolic beach terminates the basin.

The float is a vertical cylinder of 0.5 m diameter and 0.25 m height connected to a hemispherical hull of 0.5 m diameter. It has a dry mass of 43.2 kg and is moored with a single taut mooring attached to the bottom of the hemisphere. The mooring is made from Dyneema® rope (spring constant, $k \approx 35\text{N/mm}$) in series with a linear spring ($k = 0.064\text{ N/mm}$) which provides the mooring's extension. The minimum and maximum lengths of the spring are 152 mm and 406 mm respectively. Four lengths of rope act as end stops for the spring, preventing it from being extended past its elastic limit. A load cell is located in series with the mooring while an optical tracking system was used to record the motion of the float.

A wave probe was placed at the focus location (20.65 m from the paddles) without the float in place. The theoretical focus location of the zero phase wave was then adjusted using a trial and error process (Ning et al [5]) until the required wave group symmetry was obtained. This theoretical focus location was then assigned to all other wave groups tested.

3 Stokes-type expansion

The linear combination of wave groups to separate the linear and nonlinear harmonics of surface elevation (η) is based on a Stokes-type expansion of the surface elevation, which to 4th order gives:

$$\eta(\theta) = \eta_{11}A \cos(\theta) + \eta_{20}A^2 + \eta_{22}A^2 \cos(2\theta) + \eta_{31}A^3 \cos(\theta) + \eta_{33}A^3 \cos(3\theta) + \eta_{40}A^4 + \eta_{42}A^4 \cos(2\theta) + \eta_{44}A^4 \cos(4\theta) + O(A^5), \quad (1)$$

where A and θ are the amplitude and phase of the wave group and η_{ij} are coefficients in the expansion. It has previously been shown [1] that a linear combination of 0°, 90°, 180° and 270° phase wave groups can be used, in combination with the Hilbert transform (indicated by h), to extract the coefficients associated with different harmonics:

$$\text{1st order} \quad \eta_{11}A \cos(\theta) + \eta_{31}A^3 \cos(\theta) = \frac{1}{4} [\eta(0) - \eta(90)h - \eta(180) + \eta(270)h] \quad (2)$$

$$2^{\text{nd}} \text{ order} \quad \eta_{22}A^2 \cos(2\theta) + \eta_{42}A^4 \cos(2\theta) = \frac{1}{4} [\eta(0) - \eta(90) + \eta(180) - \eta(270)] \quad (3)$$

$$3^{\text{rd}} \text{ order} \quad \eta_{33}A^3 \cos(3\theta) = \frac{1}{4} [\eta(0) + \eta(90)h - \eta(180) - \eta(270)h] \quad (4)$$

$$\text{Combined } 0^{\text{th}} \text{ and } 4^{\text{th}} \text{ order} \quad \eta_{20}A^2 + \eta_{40}A^4 + \eta_{44}A^4 \cos(4\theta) = \frac{1}{4} [\eta(0) + \eta(90) + \eta(180) + \eta(270)]. \quad (5)$$

In the previous method [1], the 0th and 4th order terms have been separated using frequency filtering. Here an alternative set of combinations is derived using 12 different phase wave groups. Each wave group with a phase between 0° and 180° must be summed with the equivalent wave group between 180° and 360° (e.g. 30° and 330°, 60° and 300° etc.) to ensure the necessary wave components cancel over the entire time series.

$$0^{\text{th}} \text{ order} \quad \eta_{20}A^2 + \eta_{40}A^4 = \frac{1}{12} [\eta(0) + \eta(30) + \eta(60) + \eta(90) + \eta(120) + \eta(150) + \eta(180) + \eta(210) + \eta(240) + \eta(270) + \eta(300) + \eta(330)] \quad (6)$$

$$1^{\text{st}} \text{ order} \quad \eta_{11}A \cos(\theta) + \eta_{31}A^3 \cos(\theta) = \frac{1}{2\sqrt{3}} [\eta(30) + \eta(330) - \eta(150) - \eta(210)] \quad (7)$$

$$2^{\text{nd}} \text{ order} \quad \begin{aligned} \eta_{22}A^2 \cos(2\theta) + \eta_{42}A^4 \cos(2\theta) \\ = \frac{1}{4} [\eta(30) + \eta(330) + \eta(150) + \eta(210) - \eta(60) - \eta(300) \\ - \eta(120) - \eta(240)] \end{aligned} \quad (8)$$

$$3^{\text{rd}} \text{ order} \quad \begin{aligned} \eta_{33}A^3 \cos(3\theta) = \frac{1}{4} \left(\eta(120) + \eta(240) - \eta(60) - \eta(300) \right. \\ \left. + \frac{1}{\sqrt{3}} [\eta(30) + \eta(330) - \eta(150) - \eta(210)] \right) \end{aligned} \quad (9)$$

$$4^{\text{th}} \text{ order} \quad \eta_{44}A^4 \cos(4\theta) = \frac{1}{4} [\eta(0) + \eta(90) + \eta(180) + \eta(270)] - RHS(Eqn. (6)) \quad (10)$$

These alternative combinations avoid the need for frequency filtering to split the 0th and 4th order terms and remove the need to use the Hilbert transform. They also provide a means to check the quality of the experimental data and the validity of the linear combinations method; the two sets of combinations to extract the 1st, 2nd and 3rd order terms do not use any of the same wave groups. As such the difference between, for example, the 1st order terms calculated using Eqn. (2) and Eqn. (7) gives a measure of the consistency of this procedure.

4 Wave measurements

The harmonics of the measured surface elevation, extracted using Eqns. (6) to (10), are plotted together in Figure 1 and individually in Figure 2 with vertical scales adjusted between plots. The 1st order term, which is dominated by the linear term η_{11} , is the largest component indicating that the wave groups are only weakly non-linear. A significant second order term can be observed, while the 3rd and 4th order terms make a much smaller contribution. The 0th order term represents the wave set-down.

The 1st, 2nd and 3rd harmonics calculated from Eqns. (2), (3) and (4) are also plotted in Figure 2 for comparison. Results from the two approaches are similar with a RMSE (root mean square error) calculated between $t = -2$ and 2 sec of 8.4×10^{-5} , 4.5×10^{-5} and 5.2×10^{-5} m. The differences observed in the 1st and 3rd harmonic are believed to be due to differences in the treatment of the 5th order terms. Expanding Eqn. (1) to 5th order (Fenton [6]) gives

$$\eta(\theta) = RHS(Eqn. (1)) + \eta_{51}A^5 \cos(\theta) + \eta_{53}A^5 \cos(3\theta) + \eta_{55}A^5 \cos(5\theta) + O(A^6). \quad (11)$$

Applying this to, for example, the two sums which isolate the 3rd order harmonic gives, for Eqn. (4):

$$\frac{1}{4} (\eta(0) + \eta(90)h - \eta(180) - \eta(270)h) = \eta_{33}A^3 \cos(3\theta) + \eta_{53}A^5 \cos(3\theta) \quad (12)$$

and for Eqn. (9):

$$\begin{aligned} \frac{1}{4} \left(\eta(120) + \eta(240) - \eta(60) - \eta(300) + \frac{1}{\sqrt{3}} (\eta(30) + \eta(330) - \eta(150) - \eta(210)) \right) \\ = \eta_{33}A^3 \cos(3\theta) + \eta_{53}A^5 \cos(3\theta) - \eta_{55}A^5 \cos(5\theta). \end{aligned} \quad (13)$$

Hence the difference between the two approaches is the 5th order harmonic ($\eta_{5,5}A^5\cos(5\theta)$). Finding the difference between Eqn. (12) and (13) provides a method to extract the 5th order harmonic.

5 Float response

The float's response to the wave groups shows a strong dependence on the group's phase. This dependence is partially dependent on the amplitude of the group's main wave crest. The input NewWave amplitude (A_n) is only expected for 0° phase. As phase increases up to 180°, the theoretical amplitude of the largest crest decreases. At 180° two crests of equal amplitude are expected. The amplitude of the largest crest then increases again as phase is increased between 180° and 360°. The maximum heave experienced by the float corresponds in all cases to the largest wave crest. In Figure 3 the amplitude of the maximum heave is plotted against the largest measured crest amplitude. A hysteresis like relationship is observed, with wave groups having phases larger than 180° generating larger values of heave for the same crest amplitude.

As would be expected, an even more significant hysteresis-like relationship is observed between the maximum surge and central crest amplitude in Figure 4. This demonstrates the influence that the previous displacement of the float has on the heave and surge generated directly by the largest crest. For example the crest amplitudes at 90° and 240° were approximately equal; however the preceding surface elevation is significantly different, and so the positions of the front face of the float is different when the largest crest arrives.

In Figure 5 the above linear combinations are applied to the float's heave to separate linear and non-linear components. The two approaches for calculating the linear component are approximately consistent. However this is not the case for the 2nd and 3rd order harmonics. This demonstrates the benefit of having two independent series of focused wave result combinations to assess the validity of this technique. It is believed that the effect of the displacement of the float from the wave focus location, as demonstrated by the hysteresis-like dependence of the float's motion on focused wave phase, along with the presence of mooring snatch loading, makes using linear combinations of focused wave measurements invalid in this case.

6 Conclusions

A new set of linear combinations of different phase focused wave groups is presented, which for the 1st, 2nd and 3rd harmonics utilise previously unused phases. By comparing results from this new set and those used by [1] and [2] a measure of validity of the linear combinations technique can be made. This new set also allows the separation of 0th and 4th order terms without the need for frequency filtering. Finally the 1st and 3rd order schemes in the two sets of combinations differ when expanded to 5th order. Combining the two therefore allows the 5th order coefficients to be extracted.

Acknowledgements

This work is supported by the EPSRC SuperGen UKCMER marine energy research consortium, through grant EP/K012487/1.

References

- [1] Fitzgerald, C., Grice, J., Taylor, P.H., Taylor, R.E., Zang, J., 2012. Phase Manipulation and the Harmonic Components of Ringing Forces on a Surface-Piercing Column. *IWWWFB27*.
- [2] Siddorn, P.D., 2012. Efficient numerical modelling of wave-structure interaction, PhD thesis, University of Oxford.
- [3] Tromans, P.J., Anaturk, A., Hagemeyer, P., 1991. A new model for the kinematics of large ocean waves: Application as a design wave. Proc. 1st Int. Conf. Offshore and Polar Engineering, Edinburgh UK, 3, pp. 64-71.
- [4] Halcrow, 2006. South west England regional development agency: Wave Hub development and design phase coastal processes study report.
- [5] Ning, D.Z., Zang, J., Liu, S.X., Eatock Taylor, R., Teng, B., Taylor, P.H., 2009. Free-surface evolution and wave kinematics for nonlinear uni-directional focused wave groups. *Ocean Engineering*, 36, pp. 1226-1243.
- [6] Fenton, J.D. 1985. A fifth-order Stokes theory for steady waves. *J. Waterway Port Coastal and Ocean Div. ASCE*, 111, pp. 693-718.

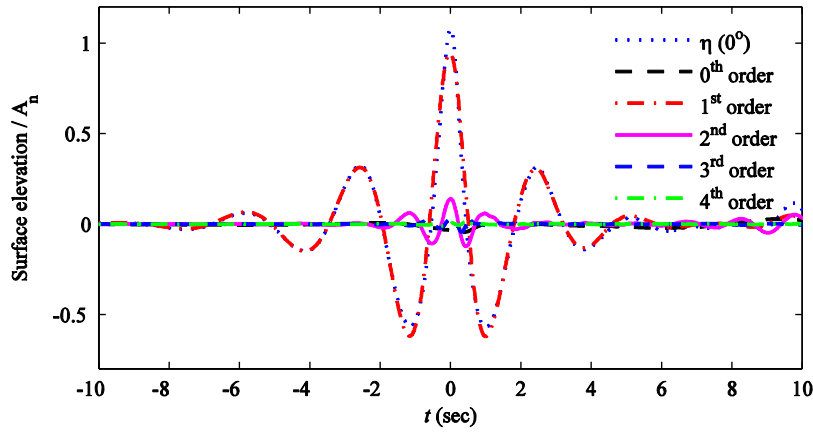


Figure 1. Harmonic decomposition of surface elevation at focus location.

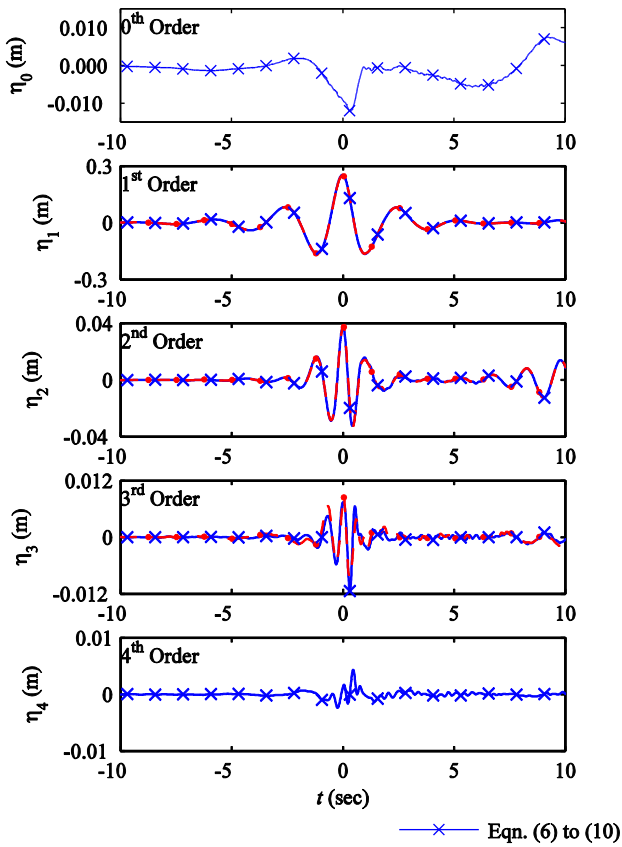


Figure 2: Individual harmonics of the surface elevation.

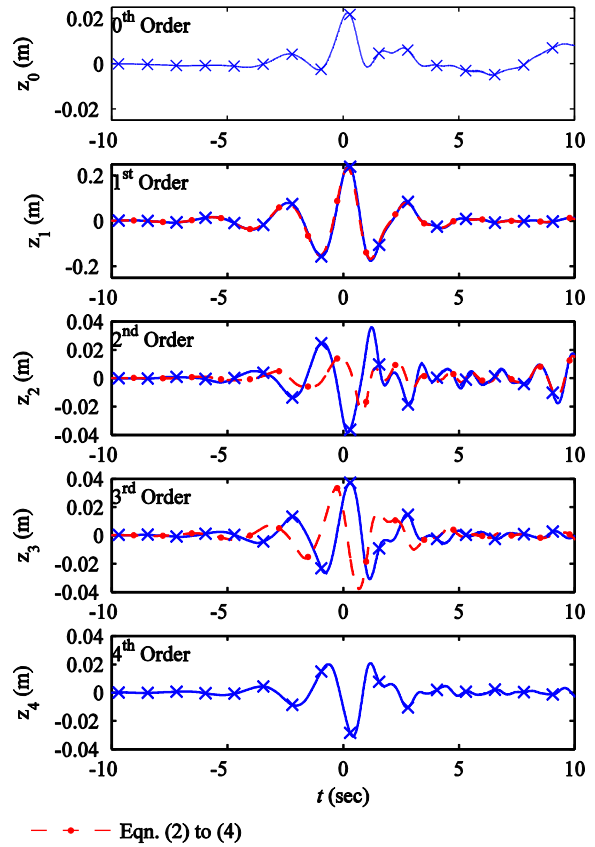


Figure 5: Individual harmonics of float heave.

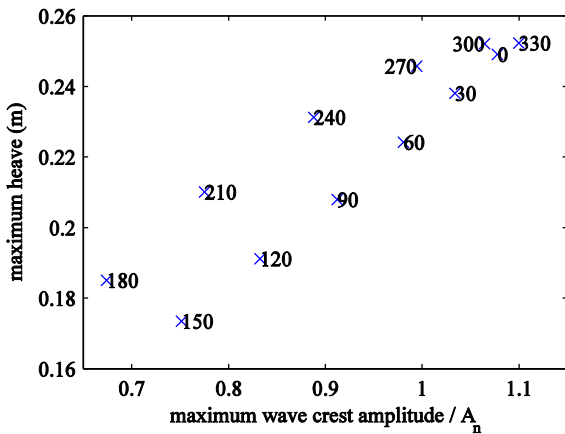


Figure 3: Maximum float heave against maximum wave crest elevation.

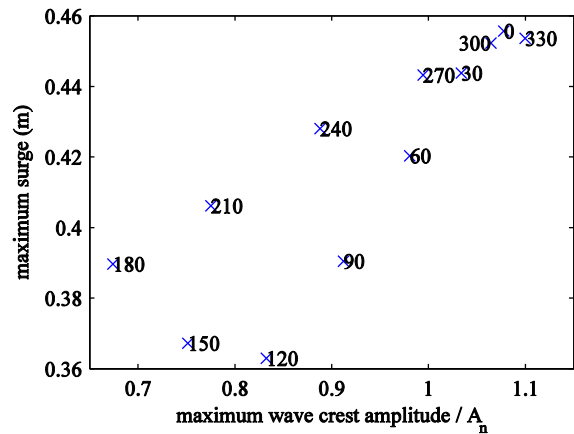


Figure 4: Maximum float surge against maximum wave crest elevation.